SINR Tight Lower bound for Asynchronous OFDM-based Multiple-Access Networks

Yahia Medjahdi⋆, Mustapha Amara† and Jérôme Louveaux⋆

†EURECOM, Campus SophiaTech,
450 Route des Chappes, CS 50193
06904 Biot Sophia Antipolis cedex, France
mustapha.amara@eurecom.fr

⋆ICTEAM, Université Catholique de Louvain,
Place du Levant, 2,
1348 Louvain-la-Neuve, Belgium
{yahia.medjahdi,jerome.louveaux}@uclouvain.be

***Abstract*—Interference modelling is an important problem necessary to design and deploy wireless communication systems. Orthogonal frequency division multiplexing (OFDM) is presented as the access technique to be used for future communication systems. Therefore, it is crucial to define a quick and reliable way of estimating signal to interference plus noise ratio (SINR) for multicarrier systems.**

The most used approach is based on the power spectral density where the out-of-band radiation of the interfering signal is computed. In this paper, we show the inaccuracy of this technique and evaluate its deviation compared to the exact value. We also derive tight lower bound expression for the SINR evaluation. We finally validate the expression through simulation results.

***Index Terms*—PSD; Interference table; Time asynchronism; OFDM; Spectrum coexistence; Cognitive Radio.**

I. Introduction

Through the past years, we have witnessed a sparsification of the frequency usage. This is essentially due to the proliferation of systems with conventional static spectrum allocation. On the other hand, spectrum resources are becoming crucial to follow the exponential bandwidth requirements of today's application and the cohabitation of multiple devices such as connected object, intelligent homes and cities. In order to overcome the problem of spectrum scarcity and resource allocation, there is a growing interest in the design and development of cognitive radio [1]. In fact, this technique that consists in an opportunistic access to the available frequency resources, offers to future communication systems the ability to dynamically and locally adapt their operating spectrum by selecting it from a wide range of possible frequencies.

Multicarrier techniques have been proposed as promising potential candidates offering both, easy adaptability and opportunistic spectrum access necessary for future cognitive communication systems [2]. Orthogonal frequency division multiplexing (OFDM), is one of the most widely spread multicarrier technique. In fact, it has been integrated in multiple standards for unlicensed wireless such as IEEE 802.22 for cognitive communications on the TV white space [3]. Unfortunately, OFDM presents some weaknesses. In fact, it has a limited frequency resolution due to the large side lobes generated by the rectangular pulse shape. This creates high amounts of interference on the adjacent bands of coexisting systems.

Moreover, due to various factors, e.g., propagation delays, spatial user distribution and timing asynchronism inter-system asynchronous interference is generated. This is considered as one of the most challenging issues in spectrum coexistence contexts.

Thus, interference modelling becomes an important phase, in the analysis and design of multiuser multicarrier communication systems, as it constitutes an essential tool in the development of interference mitigation techniques. This problem has been largely investigated during the last years. The most common approach used for that is based on the power spectral density (PSD) [4]–[7]. This modelling technique considers the out-of-band radiation determined by the PSD model of multicarrier signals. However, this model does not always give accurate results. For example, in multiuser CP-OFDM when timing offset does not exceed the cyclic prefix duration, the interference comes only from the same subchannel and the other subchannels do not contribute to this interference. Unfortunately, in this case, the PSD modelling still shows that the other carriers contribute in the resulting interference.

In this paper, the impact of asynchronous interference on the performance of OFDM systems is addressed. As a matter of fact, we:

- Analytically compare the PSD-based SINR evaluation and the real SINR value.
- Propose an accurate analytical lower bound in the case of a single subcarrier interfered by a single and multiple interfering subcarriers.
- Extend the SINR lower bound to the case of multiple interfered subcarriers.
- Evaluate the accuracy of the proposed lower bound through different simulation results.

The rest of this paper is organized as follows. Section II presents the considered system model. In Section III, we analyse in a first part the SINR and compare the PSD-based SINR evaluation to the real SINR value. In the second part, we derive a more accurate lower bound for both single and multiple interfering subcarriers. Next, we perform simulations to validate the theoretical results and expressions. We also empirically extend the lower bound to multiple interfered subcariers in Section IV. We finally conclude the paper in Section V.

II. System Model

In this paper, we consider two communicating systems, the primary (blue) and the secondary (red) coexisting in the same area. and sharing the same spectral bands.

We denote by d_1 the distance between the primary terminal (PU) and the secondary base station (SBS) with a coverage radius of R. The secondary interfered user (SU) is situated at d_0 from its base station (SBS) as shown on figure Fig. 1.a.

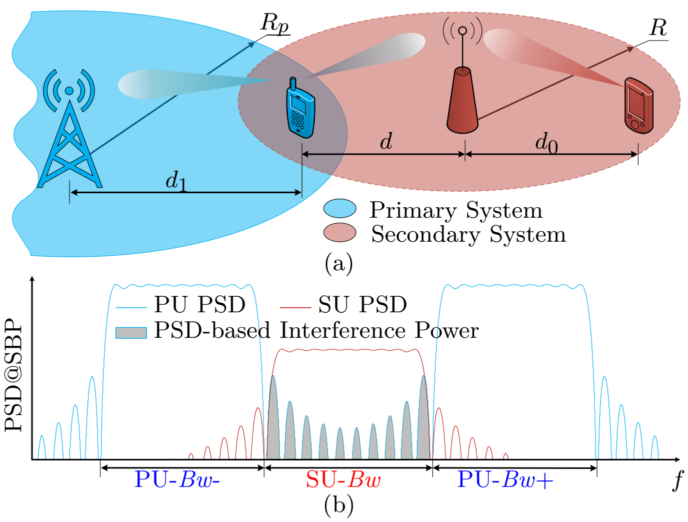

Fig. 1: Interference model: the reference user coexists with an asynchronous interferer.

Both users transmit asynchronously in adjacent bands with powers P_P and P_S respectively. The asynchronism may cause a loss of orthogonality thus leading to asynchronous interference in the SU band. This interference is represented in Fig. 1.b with the full blue lobes present appearing in SU-Bw.

In the next section we analyse the SINR at the secondary base station (SBS). It nevertheless remains valid for the primary system as well.

III. SINR Anlaysis

In this section, we analyse the average SINR considering both models: Instantaneous interference tables and PSD-based interference one. For simplicity sake, we consider flat fading propagation channels. Since the interfering signal is weighted by a complex Gaussian variable (complex channel gain), the resulting interference signal is conditionally Gaussian (for a fixed timing offset) with a variance

$$\sigma_I^2(\tau,l) = d_1^{-\beta} P_p I(\tau,l) \tag{1}$$

where β is the path-loss exponent and d_1 is the distance between the interferer and the victim receiver. We recall that l denotes the spectral distance between the interfering subcarrier and the victim one and that the timing offset between the reference receiver and the interferer is τ. The instantaneous SINR can thus be written as follows,

$$\begin{aligned}\mathrm{SINR}(\tau,l) &= \frac{d_0^{-\beta}|H_0|^2 P_s}{\sigma_{noise}^2 + \sigma_I^2(\tau,l)} = \frac{d_0^{-\beta}|H_0|^2 P_s}{\sigma_{noise}^2 + d_1^{-\beta} P_p I(\tau,l)} \\ &= \frac{|H_0|^2}{\frac{\sigma_{noise}^2}{d_0^{-\beta}P_s} + \frac{P_p}{P_s}\left(\frac{d_1}{d_0}\right)^{-\beta} I(\tau,l)}\end{aligned} \tag{2}$$

It is worth noticing that the inverse average SNR in the interference-free case is $\mathrm{SNR}^{-1} = \frac{\sigma_{noise}^2}{d_0^{-\beta}P_s}$. Thus, we obtain,

$$\mathrm{SINR}(\tau,l) = \frac{|H_0|^2\,\mathrm{SNR}}{1+\mathrm{SNR}\frac{P_p}{P_s}\left(\frac{d_1}{d_0}\right)^{-\beta} I(\tau,l)} = \frac{|H_0|^2\,\mathrm{SNR}}{1+\gamma I(\tau,l)} \tag{3}$$

where $\gamma = \mathrm{SNR}\frac{P_p}{P_s}\left(\frac{d_1}{d_0}\right)^{-\beta}$.

Assuming a uniform timing offset τ on $[0, T+\Delta]$, where T is the OFDM symbol period and Δ is the CP (cyclic prefix), we can derive the average SINR,

$$\mathrm{SINR}(l) = \frac{1}{T+\Delta}\int_0^{T+\Delta} \frac{|H_0|^2\,\mathrm{SNR}}{1+\gamma I(\tau,l)} d\tau \tag{4}$$

Following [8], the instantaneous interference tables when $l \neq 0$ are given by,

$$I(\tau,l) = \begin{cases} 0 & \tau \in [0,\Delta] \\ 2\frac{\sin^2(\pi l(\tau-\Delta)/T)}{(\pi l)^2} & \tau \in [\Delta, T+\Delta] \end{cases} \tag{5}$$

A. Single interfering subcarrier case

Accordingly, the average SINR can be rewritten as,

$$\mathrm{SINR}(l) = \frac{|H_0|^2\,\mathrm{SNR}}{T+\Delta}\left[\Delta + \int_\Delta^{T+\Delta} \frac{1}{1+\frac{2\gamma}{(\pi l)^2}\sin^2(\pi l(\tau-\Delta)/T)} d\tau\right] \tag{6}$$

Applying two successive variable changes $\tau' = \tau - \Delta$ and $x = \pi l \tau'/T$, the expression becomes

$$\mathrm{SINR}(l) = \frac{|H_0|^2\,\mathrm{SNR}}{T+\Delta}\left[\Delta + \frac{T}{\pi l}\int_0^{\pi l} \frac{1}{1+\frac{2\gamma}{(\pi l)^2}\sin^2 x} dx\right] \tag{7}$$

Since $\sin^2 x$ is even and periodic with period π, the average SINR for one interfering subcarrier becomes,

$$\mathrm{SINR}(l) = \frac{|H_0|^2\,\mathrm{SNR}}{T+\Delta}\left[\Delta + \frac{2lT}{\pi l}\int_0^{\pi/2} \frac{1}{1+\frac{2\gamma}{(\pi l)^2}\sin^2 x} dx\right] \tag{8}$$

In order to compute the final expression of the average SINR, we recall that [9, eq.436.5],

$$\int \frac{dx}{a^2+b^2\sin^2 x} = \frac{\arctan \frac{\sqrt{a^2+b^2}\tan x}{a}}{a\sqrt{a^2+b^2}}, \quad a>0 \tag{9}$$

and consequently,

$$\begin{aligned}\mathrm{SINR}(l) &= \frac{|H_0|^2\,\mathrm{SNR}}{T+\Delta}\left[\Delta + \frac{2T}{\pi}\frac{1}{\sqrt{1+\frac{2\gamma}{(\pi l)^2}}}\right.\\ &\quad \left.\arctan\left(\sqrt{1+\frac{2\gamma}{(\pi l)^2}}\tan x\right)\right]_{x=0}^{\pi/2}\\ &= \frac{|H_0|^2\,\mathrm{SNR}}{T+\Delta}\left[\Delta + \frac{T}{\sqrt{1+\frac{2\gamma}{(\pi l)^2}}}\right] \end{aligned}\tag{10}$$

Similarly to (3), the PSD-based SINR is given by,

$$\mathrm{SINR}_{PSD}(l) = \frac{|H_0|^2\,\mathrm{SNR}}{1+\gamma I_{PSD}(l)} \tag{11}$$

where, the PSD-based interference table coefficient corresponding to a spectral distance of l subcarriers with a band width of Δf is equal to,

$$\begin{aligned} I_{PSD}(l) &= \int_{(l-1/2)\Delta f}^{(l+1/2)\Delta f} \phi(f)df \\ &= \left[\frac{\mathrm{Si}\left(2\pi f(T+\Delta)\right)}{\pi(T+\Delta)} - f\mathrm{sinc}^2(\pi f(T+\Delta))\right]_{f=\frac{l-\frac{1}{2}}{T}}^{\frac{l+\frac{1}{2}}{T}} \end{aligned}\tag{12}$$

as $\phi(f)$ in the OFDM case is given by

$$\phi(f) = T\left(\frac{sin\,(\pi f T)}{\pi f T}\right)^2 \tag{13}$$

In order to compare the exact average SINR given in (10) to the PSD-based one (11), we have to solve the following

$$\mathrm{SINR}(l) - \mathrm{SINR}_{PSD}(l) = 0 \tag{14}$$

After some transformations, (14) becomes

$$\begin{aligned}2\Delta^2\alpha^2\gamma^3 + \alpha\left(4T\Delta + \alpha(\pi l)^2(T^2-\Delta^2)\right)\gamma^2 + \\ \left(2T^2 - 2T\Delta\pi^2 l^2\alpha - 2\alpha\pi^2 l^2 T^2\right)\gamma = 0\end{aligned} \tag{15}$$

where α stands for $I_{PSD}(l)$ given in (12). The roots of this equation are,

$$\begin{cases}\gamma_0 = 0\\ \gamma_1 = \frac{4T\Delta+\alpha(\pi l)^2(T^2-\Delta^2)-\pi\sqrt{\alpha l^2(T+\Delta)^2[\alpha(\pi l)^2(T-\Delta)^2+8T\Delta]}}{4\alpha\Delta^2} \geq 0\\ \gamma_2 = \frac{4T\Delta+\alpha(\pi l)^2(T^2-\Delta^2)+\pi\sqrt{\alpha l^2(T+\Delta)^2[\alpha(\pi l)^2(T-\Delta)^2+8T\Delta]}}{4\alpha\Delta^2} > 0\end{cases} \tag{16}$$

It is worth noting that, since $\alpha = I_{PSD}(l) \leq \mathbb{E}_\tau I(\tau, l)$ when $l \neq 0$, the root $\gamma_1 \geq 0$ [10] . Consequently, the sign of $\mathrm{SINR}(l) - \mathrm{SINR}_{PSD}(l)$ with respect to $\gamma = \mathrm{SNR}\frac{P_p}{P_s}\left(\frac{d_1}{d_0}\right)^{-\beta}$ is given in the following table,

γ	0		γ_1		γ_2		$+\infty$
$\mathrm{SINR}(l) - \mathrm{SINR}_{PSD}(l)$	0	+	0	-	0	+	0

TABLE I: Accuracy of the PSD-based SINR

B. *Multiple interfering subcarrier case*

As proceeded for equation (6) and using the change of variable $\tau = \tau - \Delta$, the average SINR in the case of L interfering subcarriers can be expressed in the following form,

$$\mathrm{SINR}(l) = \frac{|H_0|^2\,\mathrm{SNR}}{T+\Delta}\left[\Delta + \int_0^T \frac{d\tau}{1+\sum_{l=1}^{L}\frac{2\gamma}{(\pi l)^2}\sin^2\left(\pi l\frac{\tau}{T}\right)}\right] \tag{17}$$

Before deriving the integral of the average SINR, it is wise to compute the following sum,

$$\frac{1}{\pi^2}\sum_{k=L'}^{L+L'}\frac{\sin^2\left(k\frac{\tau\pi}{T}\right)}{k^2} = \mathrm{Re}\left\{\frac{1}{\pi^2}\sum_{k=L'}^{L+L'}\frac{\mathrm{e}^{\left(2jk\frac{\tau\pi}{T}\right)}}{k^2}\right\} \tag{18}$$

$$\begin{aligned} &= \frac{1}{\pi^2}\mathrm{Re}\left\{e^{2j\frac{\tau\pi}{T}(L+L')} \times \left(e^{-2jL\frac{\tau\pi}{T}}\Phi\left(e^{2j\frac{\tau\pi}{T}},2,L'\right) - \right.\right.\\ &\quad \left.\left.\Phi\left(e^{2j\frac{\tau\pi}{T}},2,L+L'\right) + \frac{1}{(L+L')^2}\right)\right. \end{aligned}\tag{19}$$

where $\Phi(z,s,a)$ is the LerchPhi function [11] and $j=\sqrt{-1}$. This expression of the interference component can only be numerically evaluated as it is based on the Riemann zeta function. We thus compute an upper bound of the sum

$$\begin{aligned}\sum_{l=1}^{L}\frac{1}{(\pi l)^2}\sin^2\left(\pi l\frac{\tau}{T}\right) &= \left(\frac{\tau}{T}\right)^2\sum_{l=1}^{L}\mathrm{sinc}^2\left(\pi l\frac{\tau}{T}\right)\\ &\leq \left(\frac{\tau}{T}\right)^2\sum_{l=1}^{+\infty}\mathrm{sinc}^2\left(\pi l\frac{\tau}{T}\right) = \frac{\tau(T-\tau)}{2T^2}\end{aligned} \tag{20}$$

In fact, we can write,

$$\begin{aligned}&\sum_{n=-\infty}^{+\infty}\mathrm{sinc}^2\left(\pi\frac{\tau}{T}nT_s\right)e^{-j2\pi f n T_s}\\ &= \int_{-\infty}^{+\infty}\underbrace{\mathrm{sinc}^2\left(\pi\frac{\tau}{T}t\right)}_{g(t)}\underbrace{\sum_{n=-\infty}^{+\infty}\delta(t-nT_s)\,e^{-j2\pi f t}}_{f(t)}dt\\ &= (G*F)(f)\end{aligned} \tag{21}$$

where $G(f)$ and $F(f)$ are the Fourier transforms of $g(t)$ and $f(t)$, respectively.

$$\begin{aligned}G(f) &= (T/\tau)\mathrm{tri}(fT/\tau)\\ &= (T/\tau)\times\begin{cases}1-fT/\tau & |f|<\tau/T\\ 0 & otherwise\end{cases}\end{aligned} \tag{22}$$

$$F(f) = (1/T_s)\sum_{k=-\infty}^{+\infty}\delta(f-k/T_s) \tag{23}$$

Therefore, $(G*F)(f)$ is the sum of several replicas of $G(f)$ (triangular function of width $2\tau/T$) that are uniformly spaced by $1/Ts$. Setting $T_s = 1$, we obtain

$$\sum_{n=-\infty}^{+\infty} \text{sinc}^2\left(\pi\frac{\tau}{T}n\right) = (G*F)(0) \tag{24}$$

Since $\tau < T$, the different replicas of $G(f)$ can overlap utmost with $\tau/T = 1$. Consequently,

$$\sum_{n=-\infty}^{+\infty} \text{sinc}^2\left(\pi\frac{\tau}{T}n\right) = (G*F)(0) = G(0) = T/\tau \tag{25}$$

Due to the symmetry of $\text{sinc}^2(x)$, we get

$$1 + 2 * \sum_{n=1}^{+\infty} \text{sinc}^2\left(\pi\frac{\tau}{T}n\right) = T/\tau \tag{26}$$

which implies that,

$$\sum_{n=1}^{+\infty} \text{sinc}^2\left(\pi\frac{\tau}{T}n\right) = \frac{T-\tau}{2\tau} \tag{27}$$

According to (20), the average SINR given in (17) has a lower bound SINR^- which is defined by,

$$\begin{aligned}
\text{SINR}^- &= \frac{|H_0|^2\,\text{SNR}}{T+\Delta}\left[\Delta + \int_0^T \frac{d\tau}{1 + \sum_{l=1}^{+\infty} \frac{2\gamma}{(\pi l)^2}\sin^2\left(\pi l \frac{\tau}{T}\right)}\right] \\
&= \frac{|H_0|^2\,\text{SNR}}{T+\Delta}\left[\Delta + \int_0^T \frac{1}{1 + 2\gamma\frac{\tau(T-\tau)}{2T^2}}\,d\tau\right] \\
&= \frac{|H_0|^2\,\text{SNR}}{T+\Delta}\left[\Delta + \frac{4T\text{arctanh}\frac{\gamma}{\sqrt{\gamma(4+\gamma)}}}{\sqrt{\gamma(4+\gamma)}}\right]
\end{aligned} \tag{28}$$

Finally, the overall average SINR over an interfered band of L' subcarriers interfered by an adjacent band of L interfering subcarriers can be written as

$$\begin{aligned}
\overline{\text{SINR}} = &\frac{|H_0|^2 SNR\Delta}{T+\Delta} + \\
&\frac{|H_0|^2 SNR}{(T+\Delta)\,L'}\sum_{k=1}^{L'}\int_0^T \frac{d\tau}{1 + 2\gamma\sum_{l=k}^{L+k}\left(\frac{\sin\left(\pi l\frac{\tau}{T}\right)}{\pi l}\right)^2}
\end{aligned} \tag{29}$$

IV. Simulation

In this section, we investigate, the accuracy of the theoretical lower bound expression for the SINR. The average SINRs are plotted as a function of the distance d. The coverage areas of the primary and secondary BSs are taken as $R_p = R = 1$.

In Fig. 2 we plot the simulated average SINRs using the instantaneous tables (line) computed using (29), the PSD-based table (dashed lines) and the theoretical lower bound computed in (28) (dash-dotted lines).

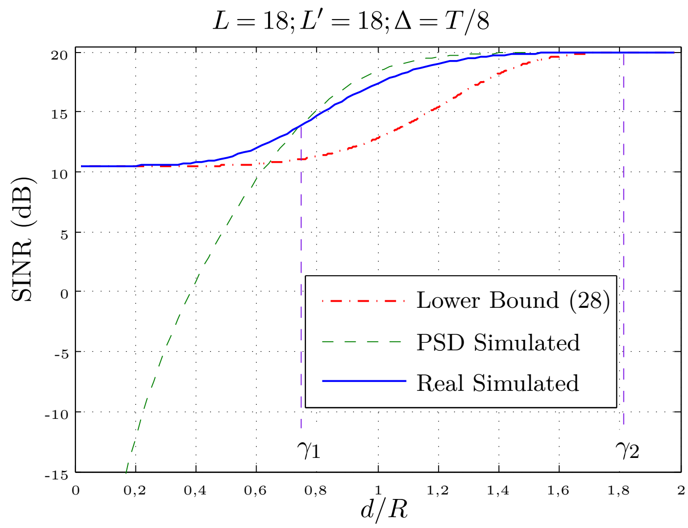

Fig. 2: OFDM average SINR *vs.* distance between PU and SBS

We mention, first of all, that these simulations validate the study performed in the first part of this paper. In fact, the curves of the PSD and instantaneous tables intersect in two points, respectively γ_1 and γ_2 given by (16).

These curves also validate the analysis result obtained in table I as the PSD-based simulation over estimate the interference in the interval $[\gamma_1, \gamma_2]$ and under estimates it elsewhere.

It is also important to mention the poor quality of the SINR estimation of the PSD-based approach especially for $d < \gamma_1$. In fact in the cognitive configuration, the error grows exponentially with the decrease of d.

On the other hand, the theoretically derived lower bound remains all the time below the real SINR level. In fact, it is perfectly accurate for $d \leq .05$ and $d \geq 1.5$. However, we note a significant gap of 5 dB in the central region. This gap can be explained by the loose upper bound used for the computation of the sum of sinc^2 in (20). It also over estimates the interference as this approximation considers the same maximal interference level for all L' interfered sub-carriers.

In order to ameliorate this closed form lower bound expression, we considered the two involved parameters L representing the number of interfering subcarriers and L' the number of interfered subcarriers in the band.

In Fig. 3, we represent the evolution of the SINR in function of d and L in the case of a single victim subcarrier (e.g. $L' = 1$) in order to evaluate the impact of L. These curves show reasonable gap lower than 2dB and decreasing with an increasing L. In fact, the variation of L induces a slope change of the middle part of the curve and slightly shifts the position of the inflection point.

As the estimation error of the average SINR does not depend much on L, we focus our attention on L' and empirically compute a multiplicative correction factor taking into account the behaviour of the truncated finite sum and

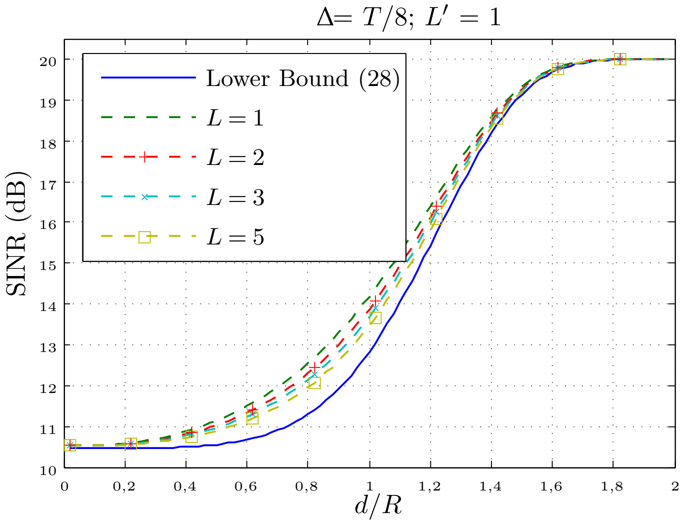

Fig. 3: Convergence of OFDM average SINR towards the lower bound (28)

the evolution of the interference contribution on each of the interfered subcarriers. Using numerical curve fitting, the obtained factor can thus be written in function of L' as

$$\gamma' = \gamma / L'^{\frac{(L')^{3/4}}{12}} \tag{30}$$

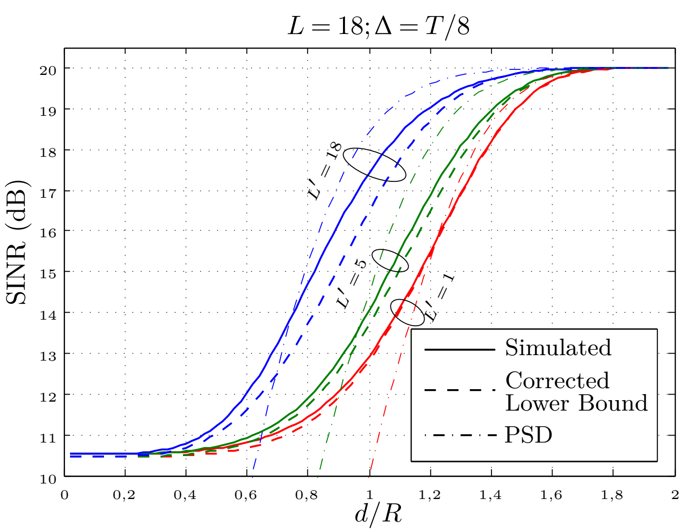

Fig. 4: Corrected SINR lower bound *vs.* average real and PSD-based SINR

These results depicted on Fig. 4 show the corrected lower bound (dashed lines) compared to the real SINR (solid lines) and the PSD-based approximation (dash-dotted lines). Analysing the solid lines and the respective dashed ones for various values of L', we observe that the PSD-based SINR evaluation under evaluates the interference levels for $d \in [\gamma_1, \gamma_2]$ and largely over estimates it for $d \leq \gamma_1$. Comparing the corrected lower bound of the SINR with the real SINR plots, one can see that the lower bound is tight as it does not exceed 1 dB in the worst case. These observations consolidate the validity of the proposed correction factor and the computed lower bound.

V. Conclusion

In this paper, we have investigated the asynchronous interference modelling in OFDM systems. We first compared the PSD-based interference to the real interference. We showed theoretically that the PSD-based method over estimates the interference in a cognitive scenario and under estimates it in the cellular configuration.

Next, we have proposed a new theoretical tight lower bound for the SINR at an interfered subcarrier in both single and multiple interfering subcarriers cases. The accuracy of this lower band has been validated through simulation results.

This SINR lower bound has then been extended to the case of multiple interfered subcarriers. We proposed a simple empirical multiplicative correction factor that has been validated through simulation.

These closed form based lower bounds offer a fast reliable and much more precise SINR evaluation compared to the PSD-based ones especially in a radio cognitive configuration.

References

[1] J Mitola J, *Cognitive radio: an integrated agent architecture for software defined radio*, PhD thesis, Royal Institute of Technology, Stockholm, Sweden, , 2000.

[2] M Bellanger M, "Physical layer for future broadband radio systems," in *Radio and Wireless Symposium (RWS), 2010 IEEE*, june 2007, pp. 436 – 439.

[3] Z Lei W Hu SJ Shellhammer W Caldwell C Stevenson, G Chouinard, "IEEE 802.22: the first cognitive radio wireless regional area network standard," in *IEEE Comm. Mag.*, 2009, pp. 130 – 138.

[4] DS Waldhauser LG Baltar and JA Nossek, *Out-of-band radiation in multicarrier systems: a comparison*, MultiCarrier Spread Spectrum vol. 1 (Springer, 2007), pp. 107–116, 2007.

[5] H. Zhang, D. Le Ruyet, and M. Terré, "Spectral Efficiency Comparison between OFDM/OQAM and OFDM based CR Networks," *Wireless Commun. and Mobile Computing Wiley*, vol. 9, pp. 1487–1501, Nov. 2009.

[6] T. Weiss, J. Hillenbrand, A. Krohn, and F.K. Jondral, "Mutual Interference in OFDM-based Spectrum Pooling Systems," in *Vehicular Technology Conference, IEEE 59th*, May 2004, vol. 4, pp. 1873–1877.

[7] M. Shaat and F. Bader, "An uplink resource allocation algorithm for ofdm and fbmc based cognitive radio systems," in *Cognitive Radio Oriented Wireless Networks Communications (CROWNCOM), 2010 Proceedings of the Fifth International Conference on*, june 2010, pp. 1 –6.

[8] Y. Medjahdi, M. Terré, D. Le Ruyet, D. Roviras, and A. Dziri, "Performance analysis in the downlink of asynchronous ofdm/fbmc based multi-cellular networks," *IEEE Trans. on Wireless Commun.*, vol. 10, no. 8, pp. 2630–2639, Aug. 2011.

[9] H. B. Dwight, *Tables of Integrals and Other Mathematical Data*, The Macmillan Company, New York, , 1957.

[10] Yahia Medjahdi, Michel Terré, Didier Le Ruyet, and Daniel Roviras, "Interference tables: a useful model for interference analysis in asynchronous multicarrier transmission," *EURASIP Journal on Advances in Signal Processing*, vol. 2014, no. 1, pp. 54, 2014.

[11] Bateman Manuscript Project, H. Bateman, and A. Erdélyi, *Higher Transcendental Functions*, Higher Transcendental Functions. McGraw-Hill, 1953.